Frame Rate Exposimetry for Pulmonary Capillary Hemorrhage During Lung Ultrasound

Douglas L. Miller, PhD 🟢 *, Chunyan Dou, MD, Zhihong Dong, MD*

Abbreviations
ALARA, as low as reasonable achievable; BMI, body mass index; CWT, chest wall thickness; FWHM, full width half maximum; IPS, image pulse sequence; LUS, lung ultrasound; MIIS, Mechanical Index in situ; MIOS, Mechanical Index on scree; PCH, pulmonary capillary hemorrhage; PRP, pulse repetition period; PRPA, peak rarefactional pressure amplitude; TI, Thermal Index

doi:10.1002/jum.16186

Objectives—Lung ultrasound (LUS) is a powerful and accessible clinical tool for pulmonary diagnosis, but risk of pulmonary capillary hemorrhage (PCH) presents a safety issue. The dependence of PCH in a rat model of LUS was evaluated for image frames-per-second (fps) and associated on-screen Mechanical Index (MI_{OS}) and Thermal Index (TI).

Methods—A Philips iE33 machine with L15-7io probe was used to scan anesthetized rats in a warmed water bath. B mode was applied at 9 MHz with settings of 34, 61 and 118 fps. After 2 minutes of exposure at an MI_{OS} setting, samples were obtained for assessment of PCH areas on the lung surface. Ultrasound parameters were measured to determine the in situ MI_{IS} at the lung surface.

Results—The PCH trend counter-intuitively decreased with increasing fps, with areas of 19.5 mm^2 for 34 fps (MI_{OS} = 1.0, TI = 0.8, 4080 images), 9.6 mm^2 at 61 fps (MI_{OS} = 1.0, TI = 0.5, 7320 images) and 7.5 mm^2 at 118 fps (MI_{OS} = 1.1, TI = 0.4, 14,160 images). The PCH was not significantly different for 34 fps (TI = 0.5, MI_{OS} = 0.8) (10.7 mm^2), compared to 61 and 118 fps, above, indicating some value for the TI as a predictive indicator of PCH. MI_{IS} thresholds were 0.42, 0.46, and 0.49 for 34, 61 and 118 fps, respectively.

Conclusions—The increase in PCH at low fps was associated with delivering more relatively high amplitude grazing pulse exposures during slower image scans. No significant PCH was found for the MI_{OS} setting of 0.5, corresponding to in MI_{IS} values of 0.35–0.39.

Key Words—B lines; bioeffects of ultrasound; Mechanical Index; neonatal lung ultrasound safety; pulmonary ultrasound; Thermal Index; ultrasound dosimetry

Introduction

Lung ultrasound (LUS) has proven to be an exceptionally powerful and readily accessible tool in neonatal care[1] and many other patient conditions.[2] LUS involves a risk of lung injury from the possible induction of pulmonary capillary hemorrhage (PCH). This finding, first reported in 1990 for pulsed ultrasound simulation of diagnostic ultrasound LUS of mouse models,[3] led to extensive research on this potential patient safety issue using laboratory pulsed ultrasound systems. In an authoritative review, the minimal threshold in terms of the Mechanical Index of exposure (determined for maximal in situ conditions at the lung) was determined to be MI_{IS} = 0.4.[4] LUS in rats with a diagnostic ultrasound machine demonstrated PCH

induction with B mode imaging at 7.6 MHz.[5] The threshold was found to be $MI_{IS} = 0.44$ for this clinical system, essentially confirming the previous findings with laboratory systems. This exposure quantity is important because the regulatory Mechanical Index is presented on screen (MI_{OS}) for many ultrasound machines, thus providing an indicator of ultrasound exposure for sonographers. Prudent of use of lung ultrasound in patients should include consideration of possible PCH occurrence and use of the recommendation that LUS should be conducted with MI_{OS} ≤0.4 or 0.3 in vulnerable patients.[6,7] Lower Mis are also suggested to avoid compromising the quality of the lung surface image due to saturation phenomena.[8] If output >MI_{OS} is needed for optimal imaging, then the practice of the As Low As Reasonably Achievable (ALARA) principal is recommended.

The mechanism of PCH induction seems to be ultrasonic radiation pressure but the detailed injurious interaction above the threshold remains uncertain.[9] The PCH bioeffect magnitude also depends on other physical parameters, such as LUS frequency[10] exposure duration,[11] and ultrasound mode.[12] Furthermore, PCH risk depends on patient physiological conditions, such as specific anesthetic techniques,[13] mechanical ventilation[14] or hemorrhagic shock.[15] The management of this risk through use of on-screen exposure indices is needed for patient safety. However, the simple use of the worst-case MI threshold may not be suitable for some LUS applications, such as high BMI patients. Above the threshold recommendation, practitioners should practice ALARA. More information on changes in PCH risk with machine setting is needed to aid in the practice of ALARA In addition, better information for use of the on-screen ultrasound exposure indices (MI and Thermal Index [TI]) is needed to allow optimum usage of LUS for patients.

In this study, the variation of PCH induction and magnitude with B mode scan rate (frames per second, fps) was investigated as an important additional exposure parameter related to exposure duration. Our hypothesis was that the PCH effect accumulates with each image such that the single MI_{OS} peak pulse for each image defines the required exposure unit. For the same MI value, higher fps settings should produce greater effect within a given exam duration, related to the total number of image-exposures delivered. The rat model of LUS was researched, with ultrasound equipment similar to that used in previous studies.[5,10,15] Results partly supported our hypothesis but also revealed an important dependence on the details of the sequence of pulses delivered for each image.

Materials and Methods

Animal Preparation

All in vivo animal procedures were conducted with the approval and guidance of the Institutional Animal Care and Use Committee (IACUC), University of Michigan, Ann Arbor, MI. Female Sprague Dawley rats were obtained from Charles River Breeding Labs (Wilmington, MA, USA) and housed by the University Unit for Laboratory Animal Medicine. The study was conducted in two parts with the first part including 110 rats, and the immediately following second part including 74 rats. The rats weighed an average of 237 ± 16 g and 246 ± 18 g at the time of testing in the first and second parts, respectively. Each rat was anesthetized with an intraperitoneal injection of ketamine (Zetamine™ ketamine hydrochloride injection, MWI, Boise, ID, USA) 91 mg/kg plus xylazine (XylaMed™ xylazine injection, MWI, Boise, ID, USA) 9 mg/kg, as recommended by the IACUC. Although xylazine is not for human use, the clinical sedative Dexmedetomidine has a similar influence on the PCH effect as xylazine.[16] For good ultrasound transmission, the right thorax of each rat was shaved and depilated. A pulse oximeter probe (Kent Scientific Inc., Torrington, CT, USA) was placed on a paw for determining heart rate, which averaged 274 ± 28 bpm and 278 ± 27 bpm, for the first and second parts, respectively, and $\%SpO_2$ which averaged $81 \pm 6\%$ and $77 \pm 7\%$ for the first and second parts, respectively. Respiration was also checked for each rat during the exposure period and averaged 67 ± 14 bpm and 72 ± 16 for the first and second parts, respectively.

Ultrasound

A Philips iE33 (Bothell, WA, USA) diagnostic ultrasound machine was used with the L15-7io probe that was a "hockey stick" linear array. The machine was used in 2D B mode General setting with 2.5 cm depth and 1.25 cm single focus. For exposure, a rat

was mounted on a plastic board which was then placed vertically in a 38°C bath filled with vacuum degassed water for exposure. This setup allowed precise aiming of the probe in the bath, while also maintaining the body temperature of the anesthetized rats. The probe was held with a gimbal mount and aimed to image through an intercostal space (parallel to the ribs) at the cranial or medial lung lobe. The nearest lung surface image was set at a depth of 1.0 cm, with deeper exposure depths following the curvatures of the lung surface. The chest wall thickness (CWT) was measured at the center point of the lung image, and averaged 4.3 ± 0.3 mm.

The iE33 had a three-position knob that changed the scan rate with RES, MID and SPD settings. At the 2.5 cm image depth and 2.3 cm width, the scan frame rates were 34, 61 and 118 fps for the RES, MID and SPD settings, respectively. The power output control knob allowed variation of the MI_{OS} with the on-screen display showing 0.1 steps with finer stops between the display steps. The ultrasound pulses and pulse sequences were measured at the position of the peak rarefactional pressure amplitude (PRPA) at 1.0 cm depth, using a calibrated hydrophone with a 0.2 mm sensitive spot (model HGL-0200, Onda Corp., Sunnyvale, CA, USA). Pulse parameters are listed in Table 1 for the different output settings used. The total number of images for the 2 minutes exposure (120×fps) is listed as valuable exposimetry parameter for his study of frame rate dependence. The center frequency was 9 MHz. The pulse waveforms for each frame rate setting are shown in Figure 1 for $MI_{OS} = 1.0$ (RES and MID) or 1.1 (SPD). The pulse shapes are slightly different, but the PRPAs (used for MI exposimetry) were all approximately equal and pulse durations calculated for the near-threshold $MI_{OS} = 0.5$ setting, with reduced finite amplitude distortion, were 157, 156 and 153 ns for the 34, 61 and 118 fps settings, respectively. The image pulses were delivered at a 62 μs pulse repetition period (PRP, or 15.6 kHz pulse repetition frequency) for all frame rate settings. The pulse PRPAs, measured in water, were derated by an attenuation factor of 1.2 dB/cm-MHz[10] over the CWT and divided by the square root of frequency to estimate the in situ MI_{IS} at the lung surface, as listed in Table 1 for the MI_{OS} settings employed. Note that the MI_{OS} values, for which an attenuation coefficient

of 0.3 dB/cm-MHz is used, are somewhat larger than the MI_{IS} values due to the greater attenuation coefficient of the CWT. The MI_{IS} is used here as the primary pulse-peak exposure parameter but the TI is also listed in Table 1 as a potentially important exposure quantity related to temporal average intensity.

The details of the measured image pulse sequences (IPS) (using a compressed time scale from Figure 1) were found to be important, and these are shown in Figure 2. Essentially, the more rapid scan rates move the beam more quickly past an alveolus on the lung surface. To illustrate this feature of the exposures, the derated rarefactional pressure amplitudes, divided by the square root of the frequency to give each pulse the units of the MI_{IS}, are compared in Figure 3 with 4 parameter Gaussian curves fitted to the plots. This comparison shows that the exposure from each IPS delivers more relatively-high amplitude indirect pulses to a point on the lung surface for the slower scan rates. An alveolus has increasing indirect exposure from the pulses as the beam approaches, a maximal pulse for direct exposure at MI_{OS} and declining indirect pulses as the beam retreats. The image was 2.3 cm in width, which was scanned by the imaging beam at a velocity given by the width times the frame rate. The lateral velocities of the swept beam were 0.78, 1.40 and 2.71 μm/μs, giving 48, 87 and 168 μm displacement between two pulse for the 62 μm PRP, for 34, 61 and 118 fps, respectively. The full-width at half-maximum (FWHM) of the Gaussian curves in Figure 3 were 1.47, 0.85 and 0.39 ms for the 34, 61 and 118 fps, respectively. These measurements provide a measure of the −6 dB beam width as the product of FWHM and the scan velocity. The average beam width estimate was 1.13 mm, about 12 times the alveolar diameter, and this was commensurate with hydrophone measurements of the thickness of the scan plane to be 1.1 mm. Dividing the FWHM by 62 μs pulse repetition period (a constant for all conditions) gives an estimate of the number of pulses within the FWHM as 24, 14 and 6 pulses for 34, 61 and 118 fps, respectively.

The second part of the study explored the effect of the same IPSs shown in Figure 2 but with frame rates varied to allow assessment of the variation of PCH with frame rate but the same IPS, see Table 1. The 34 fps IPS was reproduced with actual frame rates of 15.4 fps by using a 65 ms (trigger interval

Table 1. The Pulse Parameters Used for the 25 Exposure Settings and the PCH Area Results

| IPS Setting	MI_{OS} MPa MHz$^{-1/2}$	TI	PRPA MPa	MI_{IS} MPa MHz$^{-1/2}$	PCH mm^2	P Re sham
RES	0.9	0.6	2.40	0.80	5.6 ± 3.4	.002
34 fps @	0.8	0.5	2.08	0.69	4.9 ± 2.1 2.12.12.7.2	.001
15.4 fps	0.6	0.2	1.42	0.47	0.12 ± 0.19 0.19.	.3
TF = 1848	0.5	0.1	1.13	0.38	0	—
RES	1.0	0.8	2.60	0.87	19.5 ± 9.9	.001
34 fps @	0.8	0.5	2.21	0.74	10.7 ± 10.6	.001
34 fps	0.6	0.2	1.48	0.49	0.5 ± 1.1	.005
TF = 4080	0.5	0.1	1.12	0.37	0.2 ± 0.3	.07
RES	0.9	1.1	2.40	0.80	14.4 ± 4.9	.001
34 fps @	0.8	0.8	2.14	0.71	11.9 ± 6.2	.001
62 fps	0.6	0.4	1.48	0.49	0.9 ± 1.1	.04
TF = 7440	0.5	0.3	1.17	0.39	0	—
MID	0.9	0.4	2.39	0.80	2.3 ± 1.9	.001
61 fps @	0.8	0.3	2.07	0.69	1.0 ± 1.3	.04
33 fps	0.6	0.1	1.40	0.47	0	—
TF = 3960	0.5	0.1	1.14	0.38	0	—
MID	1.3	0.7	3.04	1.01	16.6 ± 6.3	.001
61 fps @	1.0	0.5	2.58	0.86	9.6 ± 4.3	.001
61 fps	0.8	0.3	2.14	0.71	1.6 ± 1.7	.001
TF = 7320	0.6	0.2	1.44	0.48	0.1 ± 0.3	.2
	0.5	0.1	1.17	0.39	0	—
SPD	1.1	0.4	2.52	0.84	7.5 ± 2.8	.001
118 fps@	0.8	0.2	1.80	0.60	0.3 ± 0.4	.005
118 fps	0.6	0.1	1.33	0.44	0	—
TF = 14,160	0.5	0.1	1.04	0.35	0	—

TF, total frames in 2 minutes; PRPA, peak rarefactional pressure amplitude; MI_{OS}, MI on screen; MI_{IS}, MI calculated in situ value; TI, thermal Index.
Statistical tests were two group Rank Sum tests against the sham conditions with n = 12 for the first part of the study and n = 8 for the second part (see Methods section).

Figure 1. Measured (non-derated) pulse shapes for the three fps values at MI_{OS} settings of 1.0, 1.0, and 1.1 for 34, 61 and 118 fps, respectively. Note that, although the pulse shapes are slightly different, the peak rarefactional pressure amplitudes (used for Mechanical Index exposimetry) are approximately equal.

RES 34 fps   MID 61 fps   SPD 118 fps
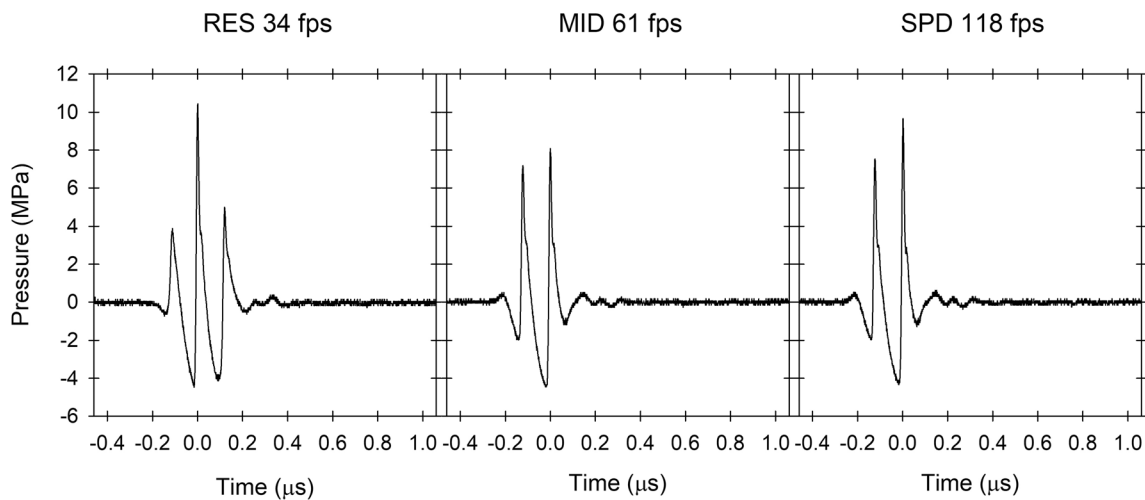
Figure 2. Measured image pulse sequences for the three fps values, as in Figure 1. The ~156 ns pulses are spaced at a repetition period of 62 μs.
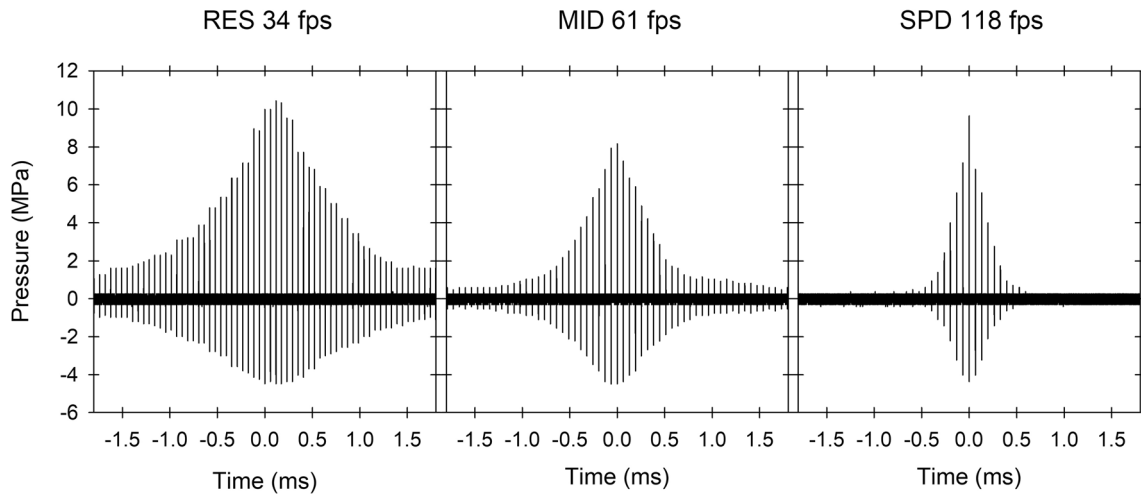
Figure 3. Measured and derated values of the rarefactional pressure amplitudes expressed as MI_{IS} values for the image pulse sequences of the three fps values (Figure 2). The slower scan rates gave broader IPS sequences with full-width at half-maximum (FWHM) values for the fitted Gaussian curves of 1.47, 0.85 and 0.39 ms for 34, 61 and 118 fps, respectively.
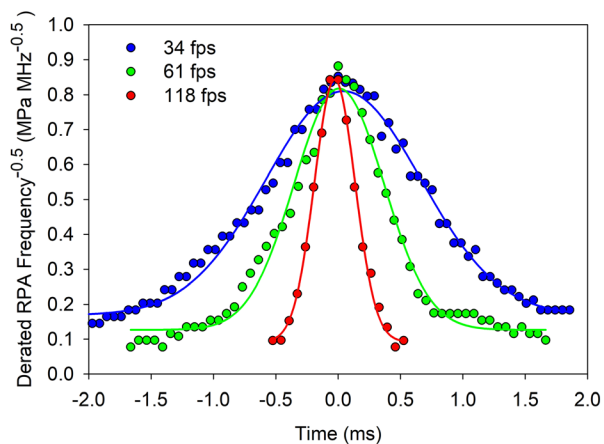
from the PHYSIO mode) and 62 fps (using the zoom feature to reduce the image width to 1.2 cm). The 61 fps IPS was produced with a 33 fps frame rate (using a 30 ms trigger interval). The exposure procedures were performed as for part 1.

Experimental Plan and Statistics
The output setting of the machine was used to adjust exposure settings for assessment of the exposure–

response trends. A 0.2 MI_{OS} was used for aiming and recording images before and after ultrasound images. For exposure to the desired setting, the MI_{OS} was quickly raised and timed for 120 seconds, after which the MI_{OS} was quickly lowered again to 0.2. During and after ultrasound exposure, the images provided a qualitative indication of developing (or not) PCH effect by displaying changes in the pleural image, such as B line artifacts. Five minutes after exposure, each rat was removed from the water bath and sacrificed under anesthesia by exsanguination of the inferior vena cava. The trachea was occluded, the thorax was opened and the heart and lungs were removed together. The right cranial and medial lobes of the lungs were examined using a stereomicroscope with digital camera (Spot Flex, Diagnostic Instruments Inc., Sterling Heights, MI, USA). Lung photomicrographs were used to measure the area of each region of PCH on the lung surface using image analysis software (Spot v. 5.1, Diagnostic Instruments Inc.). The PCH effect was limited to the scan plane (including lung sliding), with other (essentially sham exposed) lung outside the ultrasound-scanned area unaffected.

Five rats were tested each day using one famerate condition at different MI_{OS} values, as listed in Table 1. Rats were used individually with one in each condition, and this was repeated on different days until 6–7 tests had been completed for each condition. For the first part of the study, seven rats were

tested for each exposure condition plus 12 sham exposures. PCH results were unexpected: the effect *decreased* for *increasing* fps used for the 120 seconds exposures. To clarify this puzzling result, the second part of the study was planned to vary the frame rate for the same IPS in the RES and MID setting by using the zoom mode or setting the variable pulse trigger interval under the PHYSIO mode. Exposures were conducted as in part 1, with 6 rats tested in each condition plus 6 shams. The pulse and IPS parameters were maintained in part 2 for direct comparison to the results of part 1. The settings and MI_{OS} and MI_{IS} values are listed in Table 1.

Plotting of figures and statistical analysis was performed using SigmaPlot for Windows V. 14.0 (Systat Software Inc., San Jose, CA, USA). The Mann–Whitney Rank Sum test was used to compare means of measured PCH area between exposure groups and shams, and the *t*-test was used for other comparisons with statistical significance assumed at $P < .05$. The comparison of exposure results to zero PCH in sham-exposed rats tested for statistical significance of the PCH effects. Exposure-response was evaluated at MI_{OS} settings of 1.0, 0.8, 0.6, 0.5, and 0 (sham) plus 1.1 for SPD and 1.3 for MID settings. Results for these exposure-response setting were fitted for each condition by linear regression of PCH means to determine the MI_{IS} threshold (at the zero PCH intercept).

Results

The PCH results in the first part of the study showed that the high SPD frame rates were not more effective at the same MI_{OS} settings. Final ultrasound images and the PCH on the exposed lungs are shown in Figure 4 for the for $MI_{OS} = 1.0$ (RES and MID) or 1.1 (SPD) exposures. The 34 fps result was clearly greater than the 118 fps result. The PCH data is plotted in Figure 5(left) as a function of the MI_{IS}. The *reduction* in PCH with *increased* frame rate is quite dramatic, given that the number of IPSs delivered in 120 s increases from 4080 at 34 fps to 7320 at 61 fps and 14,160 at 118 fps. The exposure-response thresholds are listed in Table 2.

The second part of the study was conducted to clarify the phenomenon of decreasing PCH for increasing frame rate. As described in Methods, the 34 fps IPS was produced with varied frame rates of 15.4 and 62 fps, and the 61 fps IPS was produced with a 33 fps frame rate. The PCH results are shown in Figure 6. This data indicates that the PCH did increase with frame rate for the same IPS sequences. For the 34 fps IPS, the triggering at 15 fps involved 1848 frame-exposure, while the zoom mode with 62 fps gave 7440 frame-exposure and much greater PCH. For the 61 fps IPS, delivered at 33 fps, the number of frames was 3960, which gave less PCH than the normal 61 fps with 7320 frames of exposure (Figure 5). The thresholds for this data are listed in Table 2. These threshold values were consistent with previous work,[5] and were all approximately the same. That is, the frame rate increases maintained the threshold, associated with the approximately equal the pulse peak exposure, but varied the magnitude of PCH above the threshold.

These results suggested a role for the IPS in lung exposimetry. Examining the IPS comparison in Figure 3, the concentration of repeated pulses for the slow 34 fps scans must increase, briefly, the temporal average energy delivery. The TI, which involves the ultrasound power and temporal average intensity,[17] was used as the exposure metric for the PCH results in Figure 5(right). This exercise appeared to bring the exposure-response trends together, relative to the scattered trends shown with the for MI_{IS}. The unification by the TI was impressive additionally because the use of second-order exposure metrics (such as intensity) tend to spread data apart. For comparison to the MI_{IS} data, the thresholds for the TI are also given in Table 2.

Discussion

This study evaluated PCH induction in a rat model of LUS for different image scan rates and associated values of Mechanical Index (MI_{OS}) and soft tissue Thermal Index (TI), which are displayed on-screen to appraise the operator of ultrasound output. A Philips iE33 machine and linear array probe were used in 9 MHz B mode to assess the exposimetric dependence of PCH impact on imaging frame rate. The initial hypothesis was that increasing frame rate settings of 34, 61 and 118 fps would produce

Figure 4. Images of the post-exposure ultrasound images (top) and corresponding lung surface images (bottom). The B lines extending inward from the lung surface in the images reflect the width of the observed PCH on the middle lung lobes. Scale bars: 1 cm.
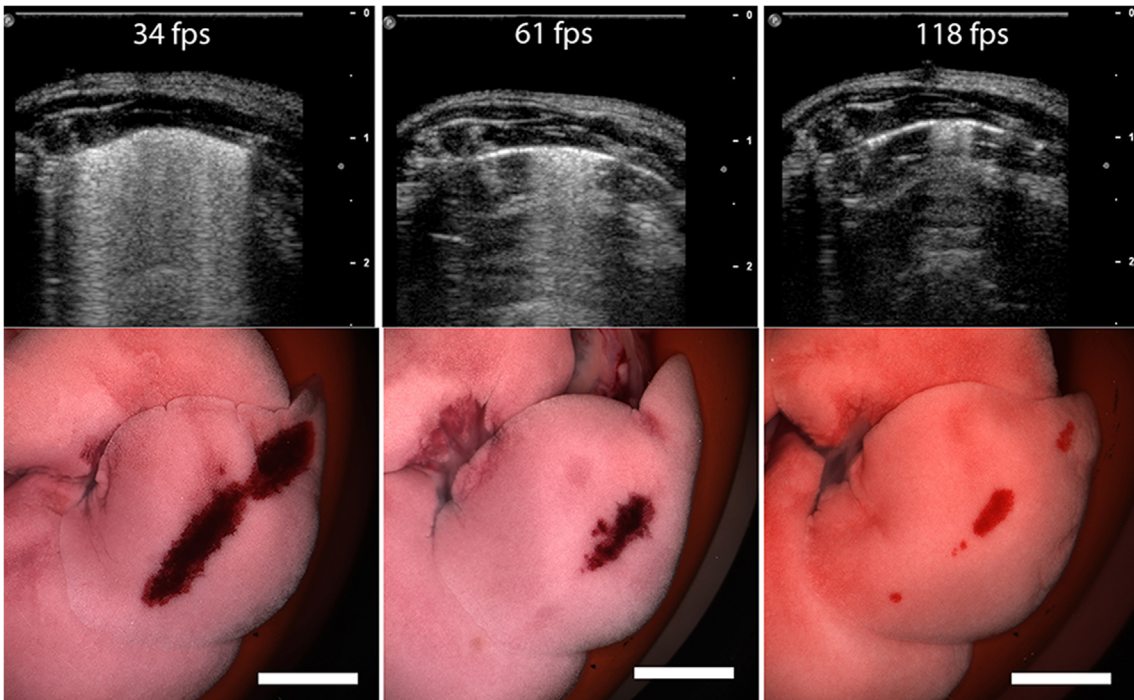
Figure 5. Results for the exposure-response PCH measurements in the first part of the study for (left) the derated Mechanical Index (MI_{IS}) and (right) the Thermal Index (TI). Use of the TI as the exposure metric here seems to bring the data plots closer together. The TI is based on the ultrasound power and intensity which are related to nonthermal mechanisms such an acoustical radiation pressure, and is not used here to indicate a thermal effect.
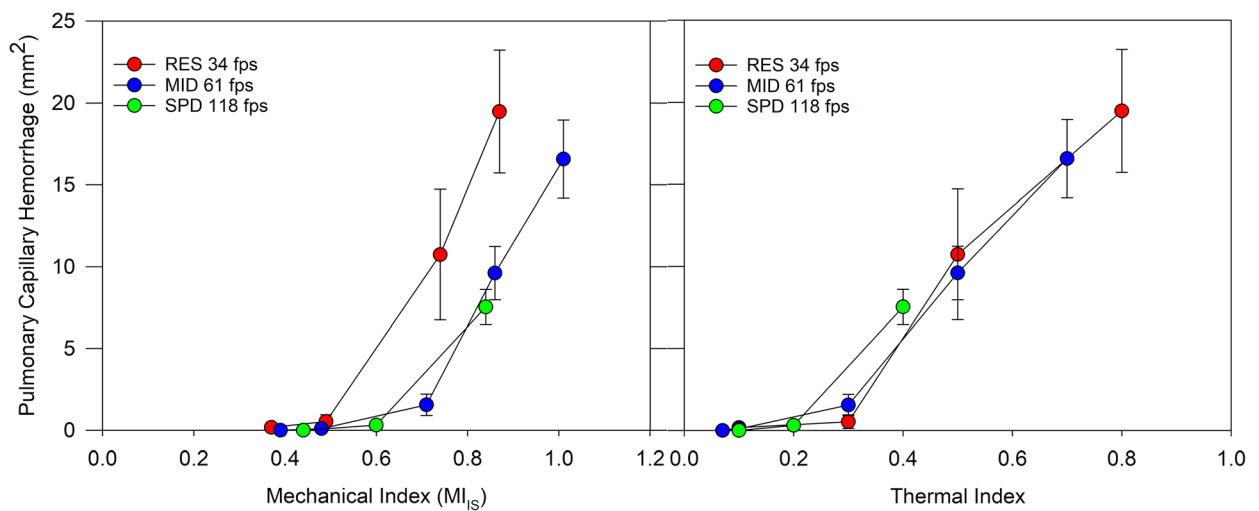
Table 2. Threshold Determinations as the Zero Crossing Point in Linear Regressions for the Exposure Response Data sets

IPS Setting	IPS (fps)	Frame Rate (fps)	Threshold MI_{IS}	r^2	Threshold TI	r^2
RES	34	15.4	0.42	0.62	0.13	0.72
RES	34	34	0.42	0.55	0.15	0.74
RES	34	62	0.40	0.73	0.12	0.74
MID	61	33	0.46	0.38	0.12	0.35
MID	61	61	0.48	0.68	0.12	0.58
SPD	118	118	0.49	0.73	0.12	0.73

The TI is used here as a surrogate index for nonthermal mechanisms such as acoustical radiation force.
MI_{IS}, MI calculated in situ.

Figure 6. Results for the PCH exposure-response measurements for the derated Mechanical Index (MI_{IS}) of exposure in the second part of the study. The magnitudes of the PCH decrease with decreasing fps for the given image pulse sequence of 34 or 61 fps reset at different actual fps values as expected, unlike the first part of the study for which PCH decreased for increased fps (Figure 5).
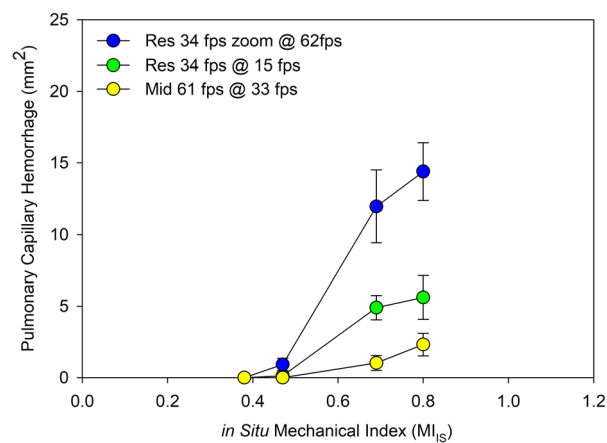
increasing PCH owing to the greater number of peak MI_{OS} pulses (one per image) in each image pulse sequences delivered during the 2 minutes tests.

Initiation and growth of B line artifacts were observed in the LUS images gave an indication of the accumulated PCH (Figure 4). PCH was zero for shams with only MI = 0.2 (TI = 0) aiming exposure. Exposure was set to specific MI_{OS} values by the output control and ultrasound parameters were measured to determine the equivalent in situ MI_{IS} actually impinging on the lung surface. For $MI_{OS} \approx 1.0$, PCH was 19.5 mm^2 ± 9.9 mm^2 for 34 fps ($MI_{OS} = 1.0$, TI = 0.8, 4080 images), 9.6 mm^2 ± 4.3 mm^2 at 61 fps ($MI_{OS} = 1.0$, TI = 0.5, 7320 images) and 7.5 mm^2 ± 2.4 mm^2 at

118 fps ($MI_{OS} = 1.1$, TI = 0.4, 14,160 images). The hypothesis of increased impact for increased frame rates was contradicted. Interestingly, the PCH was not significantly different for 34 fps (TI = 0.5, $MI_{OS} = 0.8$) with 10.7 mm^2 ± 10.6 mm^2 PCH, from the 61 and 118 fps results, Figure 5, indicating that the TI has some predictive value as an indicator of PCH magnitude. The measured MI_{IS} exposure at the lung surface was about was 80–90% of the MI_{OS}. MI_{IS} thresholds increased at 0.42, 0.46, and 0.49 for 34, 61 and 118 fps, respectively, and the magnitude was decreased substantially for increased fps. Apparent TI thresholds were 0.12–0.15; however, this observation was simply the relationship of the TI to MI numbers in this study, and does not imply that PCH was a thermal effect threshold.[18]

The results showed a counter-intuitive trend: the PCH decreased with increasing fps values, and the TI appeared to have some value as a predictive indicator of the LUS impact in this study in addition to the MI (Figure 5). However, for constant IPS, the impact does increase with increasing fps (Figure 6). The variation in PCH impact may be associated with the slower scan rates for lower fps delivering more relatively high amplitude grazing pulse exposures during the passage of the scan (Figure 3). The IPS seems to introduce some elevation of temporal average intensity, reflected in the importance of the TI (Figure 5). The data from the first part of the study are listed in Table 3 to explore the changes associated with the fps and FWHM. The PCH area declines from 19.5 to 7.5 mm^2 for 34 to 118 fps. When the PCH per fps is calculated, the dependence is clearly defined with a reduction from 0.57 to 0.064 PCH/fps for 34–118 fps. The FWHMs of 1.46, 0.87, and 0.39 ms

Table 3. Comparison of the PCH Variation with Frame Rate (fps) for the First Part of the Study with MI_{OS} at 1.0–1.1

IPS Setting	Frame Rate fps	Frames Total	PCH mm^2	PCH/fps mm^2	FWHM PN	PCH/fps-PN mm^2
RES	34	4080	19.5	0.57	24	0.024
MID	61	7320	9.6	0.16	14	0.011
SPD	118	14160	7.5	0.064	6	0.011

The PCH adjusted for the frame rate emphasizes the puzzling decrease of PCH with increase in frame number. The number of pulses (PN) within the full width at half maximum (FWHM), see Figure 3, adjusts this PCH occurrence per frame for the possible increase in exposure impact due to the slower scan rates.
MI_{IS}, MI calculated in situ.

for the 34, 61 and 118 fps settings had TIs of 0.8, 0.5 and 0.4, respectively. The TI is used here as a surrogate index for nonthermal mechanisms, such as acoustical radiation force. The number of pulses within a FWHM may be important in the higher PCH values for lower fps. That is, the PCH exposimetry is not only related to the one peak MI pulse per image, but also to the many grazing incidence pulses as the beam scans past an alveolus. The PCH per (fps-PN), where PN is the number of pulses within the FWHM, is listed in Table 3 and supports this hypothesis. The low fps seems to be compensated by the greater numbers of relatively high grazing pulse exposures in the FWHM.

These observations demonstrate fps as another machine setting, that may lead to the variation of PCH magnitude. For the practice of ALARA, the use of higher fps settings may be helpful. This feature apparently leads to so much more impact that it exceeds the expected increase in PCH with increasing fps (Table 3). This phenomenon may also depend on the PRP, which was fixed in this study. A negative result was found in a previous study of neonatal swine[19] for a GE Venue R1 machine with L4-12t probe. This setup had a fps of 29, but had a PRP of 619 μs (compare to 62 μs in this study) with an $MI_{OS} = 1.4$ and TI = 0.1. Although the fps was low, the large PRP with 8 cm image depth gave only about 3 pulses in the IPS, a factor which may help explain the puzzling negative result in that study. The PRP can sometimes be increased by using a greater image depth, another possible strategy for practicing ALARA.

More research is needed to clarify the clinical application of these findings and possibly establish an exposimetry index specifically for LUS. The use of the rat model of LUS seems removed from adult human use, due to the reduced transmission through the thicker CWTs. However, LUS in neonatal patients may have similar exposimetric conditions as rats, with a 2–8 mm range of CWT.[20] A prudent safety recommendation for neonatal LUS is to limit the B mode $MI_{OS} \leq 0.3$,[7] which could be facilitated by the creation and use of safe neonatal imaging presets.

References

1. Corsini I, Parri N, Ficial B, Dani C. Lung ultrasound in the neonatal intensive care unit: review of the literature and future perspectives. *Pediatr Pulmonol* 2020; 55:1550–1562.

2. Demi L, Wolfram F, Klersy C, et al. New international guidelines and consensus on the use of lung ultrasound. *J Ultrasound Med* 2023; 42:309–344.

3. Child SZ, Hart man CL, Schery LA, Carstensen EL. Lung damage from exposure to pulsed ultrasound. *Ultrasound Med Biol* 1990; 16:817–825.

4. Church CC, Carstensen EL, Nyborg WL, Carson PL, Frizzell LA, Bailey MR. The risk of exposure to diagnostic ultrasound in postnatal subjects: nonthermal mechanisms. *J Ultrasound Med* 2008; 27:565–592.

5. Miller DL. Induction of pulmonary hemorrhage in rats during diagnostic ultrasound. *Ultrasound Med Biol* 2012; 38:1476–1482.

6. Miller DL, Abo A, Abramowicz JS, et al. Diagnostic ultrasound safety review for point-of-care ultrasound practitioners. *J Ultrasound Med* 2020; 39:1069–1084.

7. Sande R, Jenderka KV, Moran CM, et al. Safety aspects of perinatal ultrasound. *Ultraschall Med* 2021; 42:580–598.

8. Soldati G, Smargiassi A, Inchingolo R, et al. Proposal for international standardization of the use of lung ultrasound for patients with COVID-19: a simple, quantitative, reproducible method. *J Ultrasound Med* 2020; 39:1413–1419.

9. Miller DL. Mechanisms for induction of pulmonary capillary hemorrhage by diagnostic ultrasound: review and consideration of

acoustical radiation surface pressure. *Ultrasound Med Biol* 2016; 42: 2743–2757.

10. Miller DL, Dou C, Raghavendran K. The dependence of thresholds for pulmonary capillary hemorrhage on diagnostic ultrasound frequency. *Ultrasound Med Biol* 2015; 41:1640–1650.

11. Miller DL, Dong Z, Dou C, Raghavendran K. Influence of scan duration on pulmonary capillary hemorrhage induced by diagnostic ultrasound. *Ultrasound Med Biol* 2016; 42:1942–1950.

12. Miller DL, Dong Z, Dou C, Raghavendran K. Pulmonary capillary hemorrhage induced by different imaging modes of diagnostic ultrasound. *Ultrasound Med Biol* 2018; 44:1012–1021.

13. Miller DL, Dou C, Raghavendran K. Anesthetic techniques influence the induction of pulmonary capillary hemorrhage during diagnostic ultrasound in rats. *J Ultras Med* 2015; 34:289–297.

14. Miller DL, Dong Z, Dou C, Raghavendran K. Pulmonary capillary hemorrhage induced by diagnostic ultrasound in ventilated rats. *Ultrasound Med Biol* 2018; 44:1810–1817.

15. Miller DL, Dou C, Raghavendran K, Dong Z. The impact of hemorrhagic shock on lung ultrasound induced pulmonary capillary hemorrhage. *J Ultrasound Med* 2021; 40:787–794.

16. Miller DL, Dou C, Dong Z, Raghavendran K. The influence of dexmedetomidine on ultrasound-induced pulmonary capillary hemorrhage in rats. *Ultrasound Med Biol* 2016; 42:964–970.

17. Abbott JG. Rationale and derivation of MI and TI--a review. *Ultrasound Med Biol* 1999; 25:431–441.

18. Zachary JF, Blue JP Jr, Miller RJ, Ricconi J, Eden JG, O'Brien WD Jr. Lesions of ultrasound-induced lung hemorrhage are not consistent with thermal injury. *Ultrasound Med Biol* 2006; 32:1763–1770.

19. Miller DL, Dou C, Dong Z. Lung ultrasound induction of pulmonary capillary hemorrhage in neonatal swine. *Ultrasound Med Biol* 2022; 48:2276–2291.

20. Goelz R, Krumrey S, Dietz K, Esser M, Poets CF. Safely inserting neonatal chest drains. *Neonatology* 2022; 119:33–40.